

## Second-Harmonic Current-Phase Relation in Josephson Junctions with Ferromagnetic Barriers

M. J. A. Stoutimore,<sup>1</sup> A. N. Rossolenko,<sup>2</sup> V. V. Bolginov,<sup>2,3,4</sup> V. A. Oboznov,<sup>2</sup> A. Y. Rusanov,<sup>2</sup> D. S. Baranov,<sup>2,5</sup> N. Pugach,<sup>3,6</sup> S. M. Frolov,<sup>7</sup> V. V. Ryazanov,<sup>2,4,8</sup> and D. J. Van Harlingen<sup>1</sup>

<sup>1</sup>*Department of Physics, University of Illinois at Urbana-Champaign, Urbana, Illinois 61801, USA*

<sup>2</sup>*Institute of Solid State Physics, Russian Academy of Sciences, Chernogolovka 142432, Russia*

<sup>3</sup>*Skobeltsyn Institute of Nuclear Physics, Lomonosov Moscow State University, Moscow 119991, Russia*

<sup>4</sup>*Russian National University of Science and Technology (NUST) MISiS, 4 Leninsky Prospekt, Moscow 119049, Russia*

<sup>5</sup>*Moscow Institute of Physics and Technology, Dolgoprudny 141700, Russia*

<sup>6</sup>*MIEM, National Research University Higher School of Economics, Moscow 101000, Russia*

<sup>7</sup>*Department of Physics and Astronomy, University of Pittsburgh, Pittsburgh, Pennsylvania 15260, USA*

<sup>8</sup>*Faculty of Physics, National Research University Higher School of Economics, Moscow 101000, Russia*



(Received 7 June 2018; published 26 October 2018)

We report the observation of a current-phase relation dominated by the second Josephson harmonic in superconductor-ferromagnet-superconductor junctions. The exotic current-phase relation is realized in the vicinity of a temperature-controlled 0-to- $\pi$  junction transition, at which the first Josephson harmonic vanishes. Direct current-phase relation measurements, as well as Josephson interferometry, nonvanishing supercurrent and half-integer Shapiro steps at the 0- $\pi$  transition self-consistently point to an intrinsic second harmonic term, making it possible to rule out common alternative origins of half-periodic behavior. While surprising for diffusive multimode junctions, the large second harmonic is in agreement with theory predictions for thin ferromagnetic interlayers.

DOI: [10.1103/PhysRevLett.121.177702](https://doi.org/10.1103/PhysRevLett.121.177702)

The sinusoidal dependence of supercurrent on the phase difference across the junction  $\phi$  was originally derived for superconductor-insulator-superconductor junctions but has been used to describe most of the experimentally realized junctions for a long time [1]. Advances in materials science and nanofabrication have led to the observation of a large variety of current-phase relations (CPRs) [2]. For example,  $\pi$  junctions may still have a sinusoidal CPR but with a phase shift of  $\pi$  [3–6].  $\phi_0$  junctions violate time-reversal symmetry with a phase shift  $\phi_0$  other than 0 or  $\pi$  in the CPR, meaning that their current-phase relations have no phase-inversion symmetry [7,8]. Narrow and/or ballistic weak links with nonsinusoidal current-phase relations, i.e., containing higher sine components, have been reported based on a variety of materials [9–13]. Finally, fractional current-phase relations such as  $\sin(\phi/2)$  are being searched for in topological superconductor junctions [14–16]. These developments motivate new studies of exotic CPR.

This Letter is focused on a junction with a rare second harmonic current-phase relation dominated by the  $\sin(2\phi)$  contribution. In contrast to previous studies of higher Josephson components, the junction barrier is a diffusive metal with a macroscopic number of modes. The second harmonic CPR is realized in the vicinity of a temperature-controlled 0- $\pi$  transition of a superconductor-ferromagnet-superconductor (SFS) junction. At the transition temperature  $T_\pi$  the amplitude of the first order

$\sin(\phi)$  term goes through zero in order to change sign. If a significant higher-order term is present, it can become the leading one [17]. Earlier studies of the 0- $\pi$  transition in various junctions have suggested a second-order CPR [5,18–20]; however, those experiments could not rule out alternative explanations for  $\pi$ -periodic behavior such as that due to more than one junction in the loop, disorder in the junction, or driven phase dynamics [21].

Here, we perform four distinct measurements on a single SFS junction, all four indicating a dominant and intrinsic second-order Josephson effect. First, a direct measurement of the current-phase relation is performed by embedding a single SFS junction into a superconducting loop. In this measurement, a second harmonic manifests as doubling of the superconducting loop response modulation near the 0- $\pi$  transition. Subsequently, the loop is cut and Josephson interferometry is performed on the same junction showing Fraunhofer-like patterns with half-flux quantum periodicity near  $T_\pi$ . Third, the same junction is found to exhibit a nonvanishing critical current at the 0- $\pi$  transition. Fourth, half-integer Shapiro steps are observed around the 0- $\pi$  transition. All effects are consistent with a positive  $\sin(2\phi)$  term with the critical current density of  $\approx 400$ – $600$  A/cm<sup>2</sup>. We find this to be in agreement with theory developed for diffusive junctions [22].

For the junction barrier, we use a Cu<sub>47</sub>Ni<sub>53</sub> alloy (in atomic percentage) which is a weak ferromagnet with a

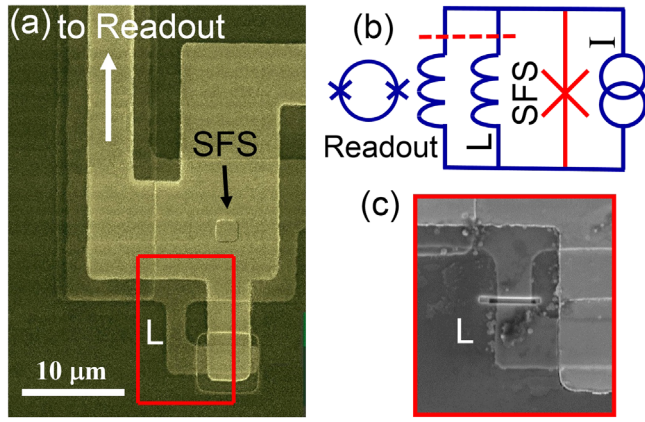


FIG. 1. (a) Optical micrograph of a prototype device, zoomed in on the area containing the trilayer SFS junction, as well as the small shunt inductor  $L$ . Red frame corresponds to the area in panel (c). (b) schematic of the CPR measurement. Dashed line indicates that both inductors are later cut to perform current-voltage measurements on the SFS junction. (c) scanning electron micrograph of the measured device, focused on the region marked by red in panel (a) after the inductor  $L$  is cut with a focused ion beam.

Curie temperature of approximately 60 K and a rigid out-of-plane domain structure [23]. SFS junctions were fabricated by depositing a Nb-CuNi-Nb trilayer in a single vacuum cycle using argon sputtering followed by multi-step fabrication process described in Ref. [24]. The junction studied in the main text has a barrier thickness of  $d_F = 7.3$  nm, and an area of  $(2 \times 2 \pm 0.5) \mu\text{m}^2$  [Fig. 1(a)]. Relative to Refs. [21,25,26], the trilayer fabrication process resulted in a lower barrier thickness of the first  $0-\pi$  transition [24], which led to the increased second harmonic amplitude.

For the direct CPR measurement, the SFS junction is shorted by a parallel combination of two superconducting Nb loops, the millimeter-scale readout loop with an inductance  $L_{\text{readout}}$  and a micron-scale loop with an inductance  $L$  [see Fig. 1(b) and the Supplemental Material [27]]. The effective inductance of the device is close to  $L$ . The readout inductor is coupled to a commercial dc superconducting quantum interference device (SQUID) sensor which detects flux  $\Phi$  in the readout loop. The bias current  $I$  is applied across the SFS junction, and inductors  $L$  and  $L_{\text{readout}}$  in parallel, it divides between the three branches to satisfy fluxoid quantization. CPR information is extracted from  $\Phi(I)$ . After performing CPR measurements, both  $L$  and  $L_{\text{readout}}$  are cut for the current-voltage measurements on the same junction [Fig. 1(c)].

The value of  $L_{\text{readout}} \approx 1.2$  nH is chosen in order to optimally couple the sample to a commercial readout SQUID. If  $L_{\text{readout}}$  were the only inductor in the circuit, the device would always be in the strongly hysteretic regime with multivalued  $\Phi(I)$  that makes it impossible to extract CPR [28]. This is due to the high critical current

density in SFS junctions with thin barriers. The small inductor  $L$  is designed to suppress the hysteresis of  $\Phi(I)$ . The single valued  $\Phi(I)$  dependence is expected for junctions with purely first-order CPR when the parameter  $\beta_{L1} = 2\pi I_{c1} L / \Phi_0 < 1$ , where  $\Phi_0$  is the superconducting flux quantum,  $I_{c1}$  is the supercurrent amplitude of the first Josephson harmonic. For a Josephson junction with a purely second harmonic CPR, the condition is more stringent:  $\beta_{L2} = 2\pi I_{c2} L / \Phi_0 < 0.5$ , so a second harmonic amplitude  $I_{c2}$  can be half as large to drive the loop hysteretic. For a generic two-component CPR, the non-hysteretic regime is obtained for  $\beta_{L2} < 16 / [(I_{c1}/I_{c2})^2 + 32]$  for  $I_{c1}/I_{c2} \leq 8$  and  $\beta_{L2} < 16 / [(I_{c1}/I_{c2}) - 2]$  for  $I_{c1}/I_{c2} \geq 8$ . (see Supplemental Material [27] for derivation).

Figure 2(a) shows the readout SQUID signal  $\Phi(I)$  for a range of temperatures that includes the  $0-\pi$  transition

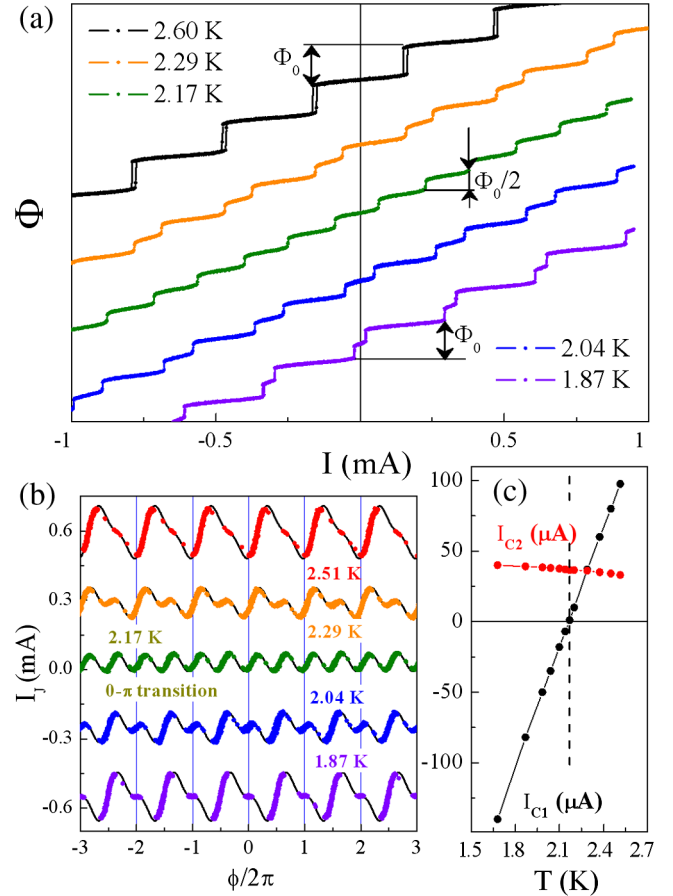


FIG. 2. (a) Readout SQUID signal  $\Phi$  as a function of  $I$  for a range of temperatures indicated in the legend.  $I$  is swept from zero to positive, then to negative, then back to zero (bipolar retrace). (b) data in panel (a) without the linear slope due to  $L$ . Black lines are fits to a two-component CPR. Curves are offset vertically. Horizontal axis scale is based on the periodicity of raw data. (c)  $I_{c1}$  and  $I_{c2}$  extracted from fits such as those in panel (a) for an extended set of temperatures. Temperature  $T_\pi$  indicated by a vertical dashed line. Solid lines are guides to the eye.

temperature  $T_\pi \approx 2.15$  K. At  $T = 2.60$  K, far above  $T_\pi$ , a sequence of equidistant steps is observed. This is typical for a weakly hysteretic superconducting loop: near each step, the magnetic flux in the loop abruptly changes by a value close to  $\Phi_0$ , and the phase across the junction changes by a value close to  $2\pi$  (see Supplemental Material [27] for a wider temperature range showing strong hysteresis). The overall slope of  $\Phi(I)$  corresponds to  $L = 6.6$  pH and is independent of temperature. At  $T = 2.29$  K the pattern acquires a double-step character, with steps half the height, i.e., close to  $0.5\Phi_0$ , occurring at uneven intervals in  $I$ . The half-steps become even in a narrow temperature range around  $T_\pi$ , as shown for  $T = 2.17$  K, resulting in half-periodic modulation of  $\Phi(I)$ . At this temperature, the CPR is purely  $\sin(2\phi)$ . The characteristics also become less abrupt and more rounded indicating that the loop is approaching the nonhysteretic regime. As the temperature is reduced below  $T_\pi$  to 2.04 K and, further, to 1.87 K, the steps are, once again, uneven indicating a growing first harmonic. The overall characteristic is shifted by half a period with respect to high temperature curves, this is because the SFS junction has transitioned into the  $\pi$  state [26].

The current-phase relation is obtained by subtracting a linear contribution due to current in  $L$ . In Fig. 2(b), we present a series of extracted CPRs within the temperature range  $1.7$  K  $< T < 2.6$  K where the condition  $\beta_{L1} < 1$  is fulfilled and half-periodicity is observable. The experimental points in Fig. 2(b) reveal the CPR for a partial range of  $\phi$  due to unexpectedly high second harmonic amplitude with  $\beta_{L2} = 0.7$  leading to weakly hysteretic  $\Phi(I)$  dependences even at  $T = T_\pi$  (see Supplemental Material [27] for details). Both amplitudes  $I_{c1}$  and  $I_{c2}$  can be extracted by fitting the experimental  $\Phi(I)$  curves assuming a two component CPR in the form  $I_J(\phi) = I_{c1} \sin(\phi) + I_{c2} \sin(2\phi)$ , where  $I_J$  is the supercurrent through the junction [Fig. 2(c)]. We see that the first harmonic crosses zero near  $T = T_\pi$ , where the CPR becomes  $\pi$  periodic. The second harmonic is weakly changing over the entire temperature range and has a positive sign. The sign of  $I_{c1}$  is fixed to be positive at higher temperatures for SFS junctions with this barrier thickness based on previous studies (Refs. [24,25], see, also, Fig. 5).

Half-periodic CPR extracted from a single-junction loop provides evidence of the dominant second harmonic that is immune to many alternative explanations. To further confirm this observation and check it against other common measurements, we cut inductors  $L$  and  $L_{\text{readout}}$  with a focused ion beam [Fig. 1(c)] and perform voltage measurements across the same SFS junction. The same readout SQUID is used but, now, in the voltmeter configuration in which  $L_{\text{readout}}$  and a small standard resistor (20 – 50 m $\Omega$ ) are shunting the SFS junction.

We find evidence of the second harmonic CPR in Josephson diffraction, by measuring the critical current

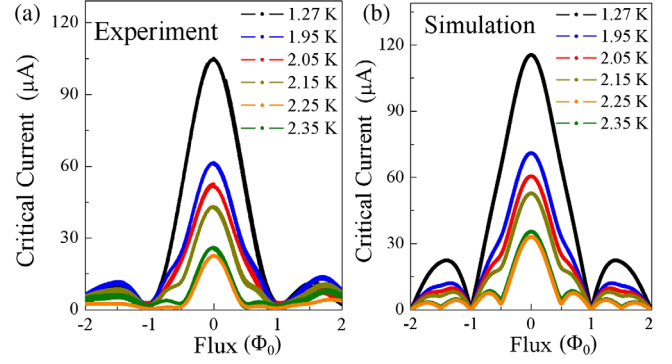


FIG. 3. (a) Experimental diffraction patterns for junction studied in Fig. 2 over a range of temperatures. The flux axis is calibrated at  $T = 4.2$  K where the data follow the Fraunhofer pattern (data not shown). (b) Simulated diffraction patterns using CPR with  $I_{c1}$  and  $I_{c2}$  from Fig. 2(c). Colors correspond to temperatures in the legend of panel (a).

as a function of flux threading the junction itself [Fig. 3(a)]. The diffraction patterns develop a second modulation near  $T_\pi$  that is half-periodic in the applied magnetic flux. This striking effect is a confirmation of the presence of a large second Josephson harmonic: indeed, in a purely  $\sin(2\phi)$  junction, the period of the diffraction pattern should be half the normal period [7,29,30]. This is most clearly seen for the applied flux in the range between  $-\Phi_0$  and  $+\Phi_0$  at  $T = 2.25$ – $2.35$  K. To confirm that such diffraction patterns can originate from a two-component CPR, we perform self-consistent simulations of diffraction patterns for a uniform junction, taking as inputs the amplitudes of  $I_{c1}$  and  $I_{c2}$  from Fig. 2(c) and allowing for a small shift in  $T_\pi$ , presumably due to the different methods of temperature measurement (see Supplemental Material [27]). The simulated curves closely reproduce the experiment [Fig. 3(b)]. The flux axis is calibrated at temperatures  $T = 1.27$  K and  $T = 2.8$  K away from  $T_\pi$ , where the diffraction patterns closely follow the Fraunhofer dependence typical for homogeneous Josephson junctions and the CPR is dominated by the first harmonic. All throughout the temperature range of the  $0$ – $\pi$  transition, the diffraction patterns exhibit a large peak in the center, at zero applied magnetic flux, thereby confirming that the junctions do not contain significant nonuniformities which would result in a zero-field minimum due to the coexistence of  $0$  and  $\pi$  regions within the junction [21,31–33].

Phase-sensitive measurements (Figs. 2 and 3) are in agreement with transport measurements (Fig. 4). The temperature dependence of the total critical current  $I_c$  for the same junction is plotted in Fig. 4(a). The data show a steady decrease of  $I_c$  as the temperature is lowered down to  $T = T_\pi$ . Below  $T = T_\pi$ , the critical current increases [3,34]. At  $T = T_\pi$ ,  $I_c$  does not reach zero, saturating at  $I_c \approx 30$   $\mu$ A. This value is consistent with  $I_{c2}$  extracted from CPR measurements.

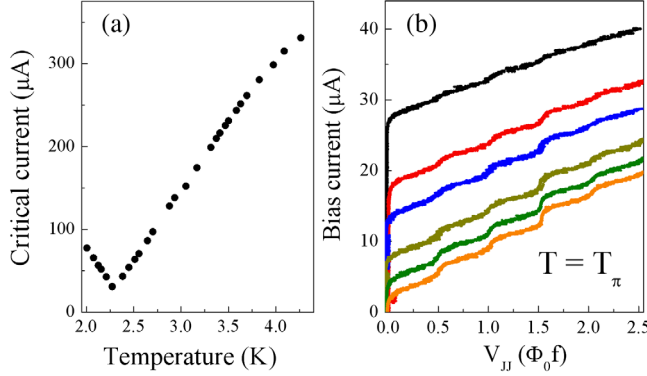


FIG. 4. (a) Critical current vs temperature for junction studied in Figs. 2 and 3. (b) Example half-integer Shapiro steps for a range of applied rf power (frequency 1.68 MHz) with black trace at lowest power and orange trace at highest applied power.

Shapiro step measurements are also commonly used to identify nonsinusoidal CPRs [15,19]. In this measurement, the junction is excited with an ac signal at frequency  $f$ . Shapiro steps appear at voltages  $V_{jj}$  equal to integer values  $nf\Phi_0$  for the first Josephson harmonic and half-integer values ( $nf\Phi_0/2$ ) for the second harmonic. Figure 4(b) shows examples of the junction current-voltage characteristics with ac excitation applied near  $T_\pi$ . There are steps at both integer and half-integer multiples of  $f\Phi_0$ . Data from additional single junction samples are presented in the Supplemental Material [27], confirming the findings. In that junction, half-integer Shapiro steps are observed in a narrow temperature range around  $T_\pi$  in agreement with previous studies [19,21].

We comment that conclusions about the second harmonic cannot be made based on the transport measurements presented in Fig. 4 alone. The nonvanishing  $I_c$  accompanied by half-integer Shapiro steps were interpreted in the past as evidence of a CPR dominated by  $\sin(2\phi)$  near  $T = T_\pi$  [19]. However, an alternative explanation for a nonvanishing critical current is due to steplike barrier inhomogeneities [21]. In this case, the junction can break into segments that have already transitioned into the  $\pi$  state and segments that remain in the 0 state. To satisfy phase continuity, supercurrents circulate in this mixed 0- $\pi$  regime around the  $F$  layer causing a nonvanishing  $I_c$ . Half-integer Shapiro steps then appear due to phase locking of these spontaneous supercurrents to the ac excitation [21,35]. Therefore, phase-insensitive measurements (Fig. 4) have to be supplemented by phase-sensitive measurements of the type presented in Fig. 2 or Fig. 3.

The last possibility to discuss is related to fine-scale barrier inhomogeneities. In this case, a junction can demonstrate diffraction patterns similar to Fig. 3(b) with a maximum critical current at zero magnetic flux, but the sign of the second harmonic is predicted to be negative [7,29,36]. This is in contrast with our measurements which have revealed a positive sign of the second harmonic. The

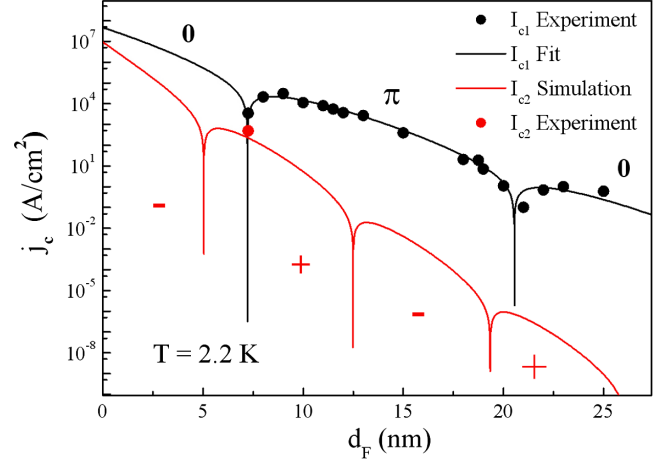


FIG. 5. Experimental barrier thickness dependence of critical current density  $j_c(d_F)$  (black circles) at  $T = 2.2$  K for junctions fabricated using the trilayer process. The data were obtained during the experiment described in Ref. [24]. The second harmonic current density from Fig. 2 is shown as a red circle. Black and red lines are fits for  $j_{c1}$  and  $j_{c2}$  based on Ref. [22]. The key fit parameters are the critical current density at zero temperature  $j_0 = 5 \times 10^7$  A/cm<sup>2</sup>, the critical current decay length  $\xi_{F1} = 1.3$  nm, and the oscillation length  $\xi_{F2} = 4.3$  nm.

positive sign is in agreement with a prediction from a microscopic theory for diffusive SFS junctions with uniform ferromagnetic barriers [22].

In order to understand the large magnitude of the second order term, we fitted the thickness dependence of the critical current density for trilayer SFS junctions to the microscopic theory [22]. In Fig. 5, the experimental data show sharp dips at barrier thicknesses  $d_F = 7.5$  and  $21.5$  nm, which are the thicknesses of the first and second 0- $\pi$  transitions. We first fitted these data assuming a purely first harmonic (black line). This allowed us to obtain the key fitting parameters. These parameters have been substituted into the analytical formula for the second harmonic [22]. The second harmonic is generally orders of magnitude smaller (red line); however, it can dominate at the first 0- $\pi$  transition. The theoretical amplitude of the second order term at  $d_F = 7.5$  nm is estimated to be  $230$  A/cm<sup>2</sup>, which is close to the experimental values (see red dot in Fig. 5). Note that the theoretical result [22] was obtained near the critical temperature of superconducting electrodes. Therefore, it cannot provide an exact quantitative agreement with the experimental value at  $T = 2.2$  K far from the niobium critical temperature.

Previous CPR measurement on a similar SFS junction [26] was performed at much larger  $d_F = 22$  nm, near the second 0- $\pi$  transition point, and showed a purely first order CPR. The second harmonic term expected from the theory in Ref. [22] for this thickness is about  $10^{-6}$  A/cm<sup>2</sup> which is too small to be measured.

In conclusion, we have demonstrated a Josephson junction with a second harmonic current-phase relation.

The regime occurs at the  $0-\pi$  transition of a superconductor-ferromagnet-superconductor junction. Alternative explanations are ruled out by comparing results from four independent methods that point at a significant  $\sin(2\phi)$  term. While the measured second-order term is surprisingly large for a diffusive SFS junction, it is in agreement with theory. The findings and methodology presented here can be used to evaluate exotic current-phase relations of other important systems, such as ballistic and topological Josephson junctions.

The authors thank N. S. Stepanov and V. N. Shilov for assistance in sample fabrication and measurements. M. J. A. S. and D. J. V. H. are supported by Grants No. NSF DMR-1710437 and No. NSF DMR-1610114. S. M. F. is supported by Grants No. NSF PIRE-1743717, No. NSF DMR-1252962, No. NSF DMR-1743972, and ONR. V. V. B. and A. N. R. are supported by Russian Foundation for Basic Research Grant No. 17-02-01270. V. V. R. is supported by the Ministry for Education and Science of Russian Federation under Contract No. K2-2014-025. N. P. gratefully acknowledges support from the TZ-93 Basic Research Program of the National Research University Higher School of Economics.

- 
- [1] B. D. Josephson, *Phys. Lett.* **1**, 251 (1962).
  - [2] A. A. Golubov, M. Y. Kupriyanov, and E. Il'ichev, *Rev. Mod. Phys.* **76**, 411 (2004).
  - [3] V. V. Ryazanov, V. A. Oboznov, A. Y. Rusanov, A. V. Veretennikov, A. A. Golubov, and J. Aarts, *Phys. Rev. Lett.* **86**, 2427 (2001).
  - [4] J. J. A. Baselmans, A. F. Morpurgo, B. J. van Wees, and T. M. Klapwijk, *Nature (London)* **397**, 43 (1999).
  - [5] J.-P. Cleuziou, W. Wernsdorfer, V. Bouchiat, T. Ondařuch, and M. Monthieux, *Nat. Nanotechnol.* **1**, 53 (2006).
  - [6] J. A. van Dam, Y. V. Nazarov, E. P. Bakkers, S. De Franceschi, and L. P. Kouwenhoven, *Nature (London)* **442**, 667 (2006).
  - [7] E. Goldobin, D. Koelle, R. Kleiner, and A. Buzdin, *Phys. Rev. B* **76**, 224523 (2007).
  - [8] D. Szombati, S. Nadj-Perge, D. Car, S. Plissard, E. Bakkers, and L. Kouwenhoven, *Nat. Phys.* **12**, 568 (2016).
  - [9] M. L. Della Rocca, M. Chauvin, B. Huard, H. Pothier, D. Esteve, and C. Urbina, *Phys. Rev. Lett.* **99**, 127005 (2007).
  - [10] I. Sochnikov, L. Maier, C. A. Watson, J. R. Kirtley, C. Gould, G. Tkachov, E. M. Hankiewicz, C. Brüne, H. Buhmann, L. W. Molenkamp, and K. A. Moler, *Phys. Rev. Lett.* **114**, 066801 (2015).
  - [11] G. Nanda, J. L. Aguilera-Servin, P. Rakyta, A. Kormányos, R. Kleiner, D. Koelle, K. Watanabe, T. Taniguchi, L. M. Vandersypen, and S. Goswami, *Nano Lett.* **17**, 3396 (2017).
  - [12] C. D. English, D. R. Hamilton, C. Chialvo, I. C. Moraru, N. Mason, and D. J. Van Harlingen, *Phys. Rev. B* **94**, 115435 (2016).
  - [13] E. M. Spanton, M. Deng, S. Vaitiekėnas, P. Krogstrup, J. Nygård, C. M. Marcus, and K. A. Moler, *Nat. Phys.* **13**, 1177 (2017).
  - [14] A. Y. Kitaev, *Phys. Usp.* **44**, 131 (2001).
  - [15] J. Wiedenmann *et al.*, *Nat. Commun.* **7**, 10303 (2016).
  - [16] R. S. Deacon *et al.*, *Phys. Rev. X* **7**, 021011 (2017).
  - [17] A. I. Buzdin, *Rev. Mod. Phys.* **77**, 935 (2005).
  - [18] J. J. A. Baselmans, T. T. Heikkilä, B. J. van Wees, and T. M. Klapwijk, *Phys. Rev. Lett.* **89**, 207002 (2002).
  - [19] H. Sellier, C. Baraduc, F. Lefloch, and R. Calemczuk, *Phys. Rev. Lett.* **92**, 257005 (2004).
  - [20] C. W. Schneider, G. Hammerl, G. Logvenov, T. Kopp, J. R. Kirtley, P. J. Hirschfeld, and J. Mannhart, *Europhys. Lett.* **68**, 86 (2004).
  - [21] S. M. Frolov, D. J. Van Harlingen, V. V. Bolginov, V. A. Oboznov, and V. V. Ryazanov, *Phys. Rev. B* **74**, 020503(R) (2006).
  - [22] A. Buzdin, *Phys. Rev. B* **72**, 100501 (2005).
  - [23] I. Veshchunov, V. Oboznov, A. Rossolenko, A. Prokofiev, L. Vinnikov, A. Rusanov, and D. Matveev, *JETP Lett.* **88**, 873 (2007).
  - [24] V. Bolginov, A. Rossolenko, A. Shkarin, V. Oboznov, and V. Ryazanov, *J. Low Temp. Phys.* **190**, 302 (2018).
  - [25] V. A. Oboznov, V. V. Bolginov, A. K. Feofanov, V. V. Ryazanov, and A. I. Buzdin, *Phys. Rev. Lett.* **96**, 197003 (2006).
  - [26] S. M. Frolov, D. J. Van Harlingen, V. A. Oboznov, V. V. Bolginov, and V. V. Ryazanov, *Phys. Rev. B* **70**, 144505 (2004).
  - [27] See Supplemental Material at <http://link.aps.org/supplemental/10.1103/PhysRevLett.121.177702> for additional data.
  - [28] A. Barone and G. Paterno, *Physics and Applications of the Josephson Effect* (Wiley, New York, 1982).
  - [29] A. Buzdin and A. E. Koshelev, *Phys. Rev. B* **67**, 220504(R) (2003).
  - [30] A. Pal, Z. Barber, J. Robinson, and M. Blamire, *Nat. Commun.* **5**, 3340 (2014).
  - [31] H. Sickinger, A. Lipman, M. Weides, R. G. Mints, H. Kohlstedt, D. Koelle, R. Kleiner, and E. Goldobin, *Phys. Rev. Lett.* **109**, 107002 (2012).
  - [32] M. Kemmler, M. Weides, M. Weiler, M. Opel, S. T. B. Goennenwein, A. S. Vasenko, A. A. Golubov, H. Kohlstedt, D. Koelle, R. Kleiner, and E. Goldobin, *Phys. Rev. B* **81**, 054522 (2010).
  - [33] J. Pfeiffer, M. Kemmler, D. Koelle, R. Kleiner, E. Goldobin, M. Weides, A. K. Feofanov, J. Lisenfeld, and A. V. Ustinov, *Phys. Rev. B* **77**, 214506 (2008).
  - [34] T. Kontos, M. Aprili, J. Lesueur, F. Genet, B. Stephanidis, and R. Boursier, *Phys. Rev. Lett.* **89**, 137007 (2002).
  - [35] C. Vanneste, C. C. Chi, W. J. Gallagher, A. W. Kleinsasser, S. I. Raider, and R. L. Sandstrom, *J. Appl. Phys.* **64**, 242 (1988).
  - [36] R. Mints, *Phys. Rev. B* **57**, R3221 (1998).